Verification of GPS III and QZSS L1C Signal Joint Positioning Performance with Software Defined Receiver

Xiang Huo[1,2], Xue Wang[1,2,3,*] , Sen Wang[1,2], Xiaofei Chen[1,2], Jing Ke[1,2]

1. National Time Service Center, Chinese Academy of Sciences, Xi'an, 710600, China

2. School of Electronic and Communication Engineering, University of Chinese Academy of Sciences, Beijing, 101408, China

3. Key Laboratory of Precision Navigation, Positioning and Timing Technology, Chinese Academy of Sciences, Xi'an, 710600, China

Xiang Huo E-mail address: 307913917@qq.com

* Corresponding author Xue Wang: Tel.: +86 18066555869, E-mail address: wangxue@ntsc.ac.cn

Abstract: Satellite navigation and positioning has become an indispensable component of smart devices and applications. In order to avoid signal interference in L1 frequency and provide novel services, Global Positioning System III (GPS III) updated a modern signal named L1C, and tested in three Quasi-Zenith Satellite System (QZSS) satellites launched in 2017. In December 2018, the first GPS III satellite was launched, which implies the joint positioning using QZSS and GPS L1C signal is improved.

L1C signal offers a series of advanced designs in signal modulation, message structure and coding, etc. In this regard, this paper presents complete methodologies for L1C signal joint receiving processing. For the on-air signals, this paper present a methodology and results from collecting and assessing Binary Offset Carrier (BOC) modulation and time-multiplexed BOC (TMBOC) modulation used in L1C signal.

Using the same omnidirectional antenna and the test-equipment, the L1C signal was collected in Xi'an and Sanya, China, respectively. Experiments in Xi'an verified the joint positioning method to complement the GPS III and QZSS satellite constellations. The methodology in this paper evaluates the positioning error of BOC(1,1) and TMBOC(6,1,4/33) under the same environment and satellite constellation in Sanya. It is also verified that the joint positioning error is less than the QZSS-only positioning due to the optimization of the satellite constellation.

Keywords: *L1C; GPS III; QZSS; Software Defined Receiver; Joint Positioning.*

Introduction

The Global Positioning System (GPS) uses radio waves to provide users with positioning, navigation, and timing (PNT) services. GPS navigation signals have numerous applications in research, industry, and everyday life [1, 2]. Civil GPS

receivers could solely use legacy L1C/A signal for positioning before GPS modernization. In 2005 and 2010, GPS broadcasted two civilian signals, L2C and L5. In 2000, the US Congress approved a plan to establish a new GPS, called GPS III. GPS III deploys a signal compatible with other Global Navigation Satellite System (GNSS) such as Galileo and QZSS at the L1 frequency, and is also the fourth generation civil signal, called L1C. The first satellite of the GPS III was launched in December 2018 [3].

The Quasi-Zenith Satellite System (QZSS) is a Japanese regional satellite positioning system. Take advantage of the high elevation of highly elliptical orbit, QZSS has been developed as a GPS-complementary system to increase the availability, reliability, integrity and accuracy of positioning performance in the Asia-Oceania region. QZS-1, the first satellite of QZSS, is in orbit since 2010. And in 2017, Japan launched three satellites to join QZSS, including QZS-2, QZS-3 and QZS-4. These four satellites transmit all GPS civil signals since the modernization of GPS, including L1C/A, L1C, L2C and L5 [4].

IS-GPS-800 [5] illustrates the L1C signal consisting of data (L1CD) and pilot (L1CP). The novel Binary Offset Carrier (BOC) modulation and time-multiplexed Binary Offset Carrier (TMBOC) modulation are used in the GPS III L1C signal, which is virtually seamless interoperability with L1C from QZSS. Up to now, there are a total of five satellites broadcasting L1C signal in orbit. A GPS III satellite with a code number of 4 is called Vespucci. The other four satellites of QZSS called QZS-1, QZS-2, QZS-3, QZS-4 use the code number 193, 194, 199, 195 respectively. It should be noted that QZS-1 differs from GPS III when it comes to modulation and phase. QZS-1 uses BOC(1,1) modulation for both data and pilot, and its pilot advances data by 90 degrees (in phase quadrature). In GPS III and three other QZSS satellites, L1CD uses BOC(1,1) modulation, and L1CP uses TMBOC(6,1,4/33) modulation. And they are in the same phase.

Combined with GPS, Yu-Hsuan Chen and his team verified that the BOC modulated signal broadcast by QZS-1 has better performance than the BPSK modulated signal in the positioning error [6]. While the anti-interference, anti-noise and other benefits of the TMBOC over the BOC have been theoretically assessed [7], but no on air, operational assessments have been published.

The research in this paper develops methods to make a direct comparison of the positioning error of TMBOC(6,1,4/33) and BOC(1,1) from GPS III and QZSS. In

view of the fact that there is barely one satellite in the current GPS III constellation, this paper proposes a joint positioning method to use GPS III for positioning service, and verified its feasibility by means of the experiments in Xi'an. The use of satellites of the same time period rather than the two periods of close proximity is the key to accurate comparison as the positioning results are sensitive to the slightest difference in the constellation geometry. Therefore, the experiments in Sanya made a detailed comparison of positioning error between the TMBOC(6,1,4/33) and BOC(1,1) modulated signals of GPS III + QZSS and QZSS-only.

Receiving and evaluation methodology

Joint positioning method

In this paper, a static test-equipment shown in Fig. 1a is used to collect signals in Xi'an and Sanya, China, which will be introduced later. The extremely high sampling rate of 250MHz and the 80MHz bandwidth of front-end filter meet the ultra-narrow correlation used in this paper. The Software Defined Receiver (SDR) used in this paper uses the L1C signal transmitted on GPS III and QZSS to processing off-line, and takes into account multiple differences in their signal structure [4, 5]. Fig. 1b is a tracking loop diagram of the SDR used in this paper. Many of its receive-related parameters are flexible and adjustable, including correlator spacing, bandwidth and damping factor for Delay Lock Loop (DLL) and Phase Lock Loop (PLL). The local signal generated by the SDR simulation for tracking is full bandwidth unfiltered. The SDR tracking method uses Bump-Jump [8], and the five pairs of correlators independently demodulate the data component and the pilot component by a coherent integration of 1 ms. The squaring operation of the non-coherent integration destroys the zero-mean of the thermal noise and brings about the squaring loss, so it is not used. Continuously tracking the carrier frequency and code phase of the L1CD demodulates the navigation massage bit stream. And the SDR demodulates the overlay code by tracking L1CP. The SDR uses the overlay code to complete the frame synchronization of the navigation message. The SDR pseudorange measurements can be selected in TMBOC(6,1,4/33) ranging and BOC(1,1) ranging. Fig. 1c is a bolck diagram of the positioning algorithm. For joint positioning, the ephemeris

needs to be modified in the algorithm to ensure that the orbit is correctly calculated.

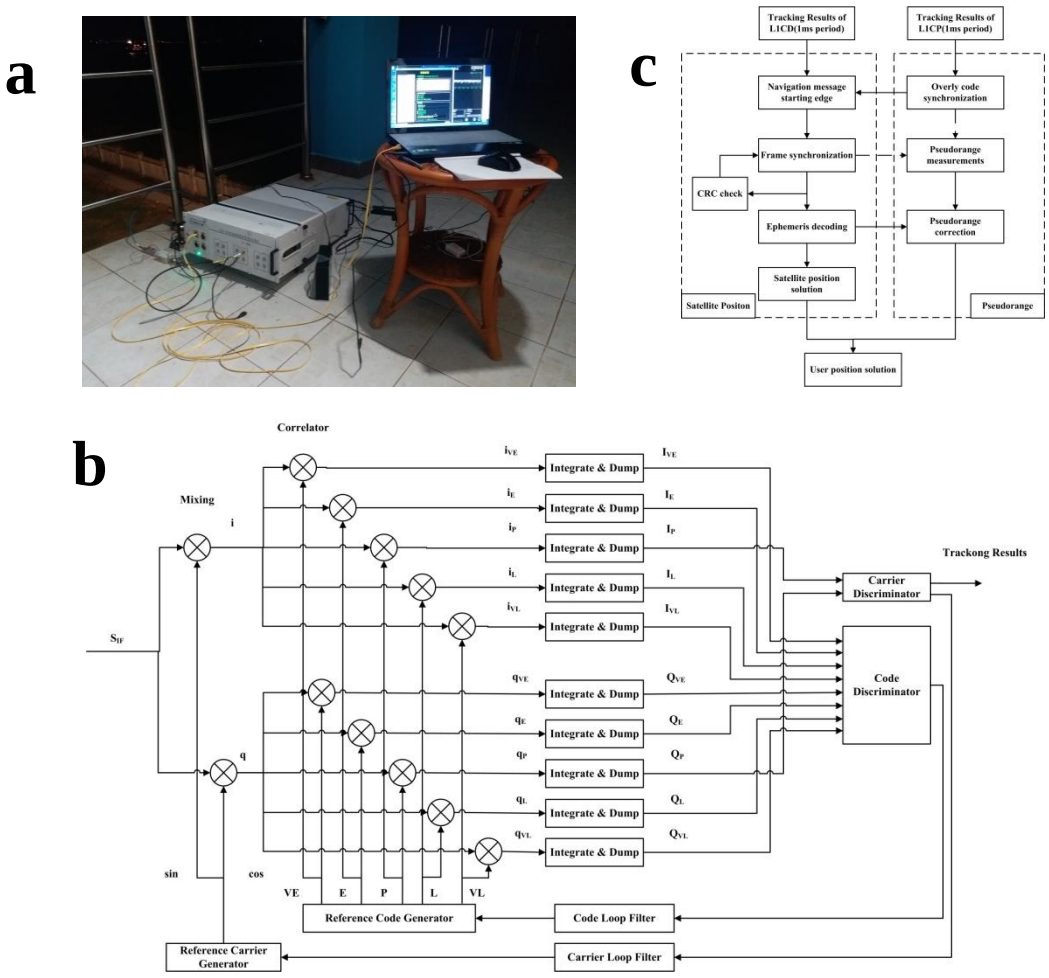

Fig. 1 The test-equipment and the SDR: **a** the test-equipment for collecting signals, **b** a representation of DLL and PLL, **c** a representation of the positioning algorithm

Positioning error

This paper uses zero baseline difference to illustrate the positioning errors of the user receivers from the reference receiver.

$$(x_n, y_n, z_n) = f(\rho_{n1}, \rho_{n2}, \dots, \rho_{nM}) \quad (1)$$

$$(x'_n, y'_n, z'_n) = (x_n, y_n, z_n) - (x_{ref}, y_{ref}, z_{ref}) \quad (2)$$

$$(x'_n, y'_n, z'_n) = \varepsilon_{\rho,n} - \varepsilon_{\rho,ref} + MP_{\rho,n} - MP_{\rho,ref} + SDM_{\rho,n} - SDM_{\rho,ref} \quad (3)$$

where $\{\rho_{nj}, j = 1, \dots, M\}$ is a set of satellite pseudorange observed by the nth user receiver, (x_n, y_n, z_n) is the three-dimensional coordinates of the nth user receiver, $(x_{ref}, y_{ref}, z_{ref})$ is the three-dimensional coordinates of the reference receiver, (x'_n, y'_n, z'_n) is the positioning error of the nth user receiver, $\varepsilon_{\rho,n}$ is

correlator-spacing dependent error at user receiver, $\varepsilon_{\rho,ref}$ is correlator-spacing dependent error at reference receiver, $MP_{\rho,n}$ is multipath error at user receiver, $MP_{\rho,ref}$ is multipath error at reference receiver, $SDM_{\rho,n}$ is nominal signal deformation error at user receiver, $SDM_{\rho,ref}$ is nominal signal deformation error at reference receiver.

Under some preconditions, the zero baseline difference can reflect the error caused by the user receiver using different correlator spacing. First, the user receivers and the reference receiver use the same satellite constellation. Second, they must use the same satellites signals. Third, their positioning algorithm must be the same. Provided that the above necessary conditions are met, the zero baseline difference can reflect the positioning error associated with the correlator spacing.

For each user which the correlator spacing is fixed, the clock error, ionosphere and tropospheric error are common mode in the positioning error equation and are therefore removed in the equation. The noise can be effectively removed with an average. In the experimental scenario below, the main residual multipath, signal nominal deformation and DLL noise are all relevant to the correlation spacing. The user receivers in this paper use different correlator spacing, including 0.1 chips, 0.15 chips, 0.175chips, 0.4 chips, which are differentiated from reference receiver with a correlator spacing of 0.05 chips.

Measurement campaign

Signal collection in Xi’an, China

QZSS satellites have elliptical geosynchronous orbit which allows them to spend a significant portion of their orbital period visible to East Asia. They provide ever present high elevation navigation signals for places such as Japan, Korea, Australia or eastern China. At present, Vespucci is in medium earth orbit and its surrounding cycle is about 24 hours, making it not visible at any time in the collection site. In southern China, Vespucci can be observed at higher elevation.

The skyplot for a user in Xi’an, China is shown in Fig. 2a. In Xi'an, the elevations of QZS-1, QZS-2, QZS-4 are sometimes less than 10 degrees or even invisible. The elevation of each satellite is greater than 10 degrees for some duration which is approximately 18 hours. Meanwhile, QZS-3 is always at about 46 degrees.

Vespucci has a total of 8 hours of elevation above 10 degrees for two periods. The trend of the elevation of Vespucci is always opposite to that of a satellite in QZSS. It should be noted that the SDR cannot use the constellation with less than four visible satellites for positioning measurement.

The signal collection site is located on the 1st floor roof of the National Time Center (NTSC) of the Chinese Academy of Sciences. The position where the omnidirectional antenna was placed is shown in Fig. 2b. Although only four satellites are visible in Xi'an, they can be used to verify the optimization of joint positioning on GPS III + QZSS constellations.

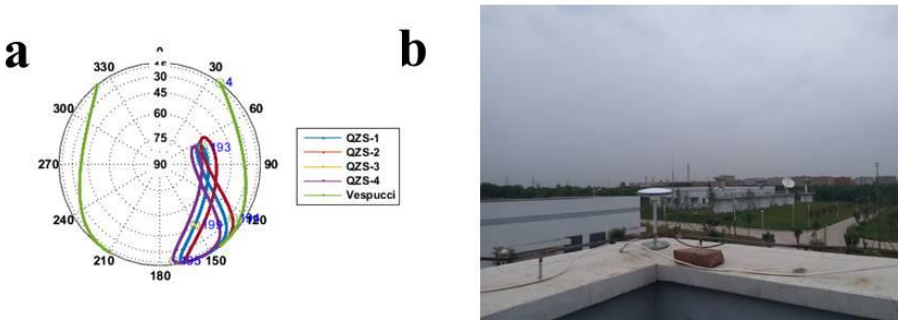

Fig. 2 Skyplot and signal collection site: **a** skyplot of GPS III and QZSS satellites with L1C observed at Xi'an, China, on January 25, 2019, with 0° elevation cutoff, **b** signal collection site at NTSC roof

Signal collection in Sanya, China

Since Sanya is in southern China, the elevation of satellites of QZSS and Vespucci of GPS III are several degrees higher than those of Xi'an. The skyplot for a user in Sanya, China observing GPS III and QZSS orbits over its 24 hours periods is shown in Fig. 3a. At Sanya, the satellites of QZSS is always visible and always significantly above 10 degrees elevation. Vespucci of GPS III is greater than 0 degrees about 12 hours. As shown in Fig. 3a, most of the dwell time, QZSS is at high elevation that greater than 45 degrees (~ 15 hours). But the trend of the elevation of Vespucci is always opposite to that of a satellite in QZSS, which is the same as in the Xi'an constellation. The signal collected in Sanya also using the test-equipment. If the constellation contains satellites with elevation below 10 degrees, the positioning results will get tremendous deterioration. So satellites collected below 10 degrees should be avoided.

The location at the hotel building by the sea was used for the signal collection. To receive GPS III and QZSS satellites signals, an omnidirectional antenna was

placed on the third floor balcony, as shown in Fig. 3b. This paper analyzes the signal collected in Sanya at UTC 12:08:10, April 13, 2019. The skyplot of the satellites visible in the course of signal collection is shown in Fig. 3c. As seen in the skyplot, GPS III and QZSS satellites are at high elevation and their direct signals could be visible at the balcony location.

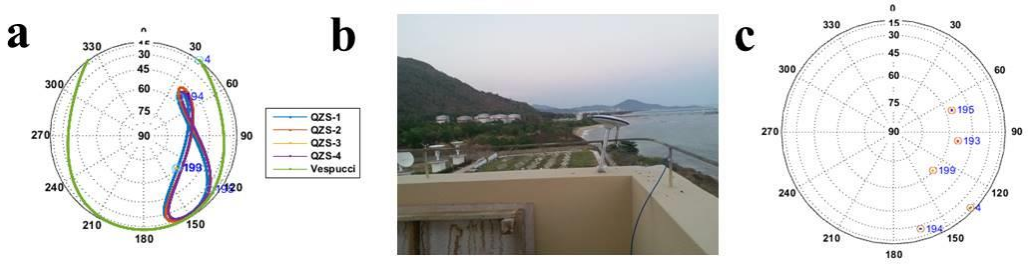

Fig. 3 Skyplot and signal collection site: **a** skyplot of GPS III and QZSS satellites with L1C observed at Sanya, China, on April 13, 2019, with 0 ° elevation cutoff, **b** signal collection site at the hotel balcony, **c** skyplot of satellites visible during GPS III + QZSS signal collection (PRN number shown)

Results

Constellation supplement effect

In order to illustrate the influence of the geometry of the satellite constellation, the positioning results of Xi'an are shown in the topocentric coordinate system. However, the positioning error of Sanya is expressed in the WGS-84 coordinate system for the purpose of clearly comparing the error.

Table. 1 Satellites visibility during two acquisition periods on January 25, 2019

Period (UTC)	Visible	Invisible
8:34:28 - 8:35:28	QZS-1, QZS-2, QZS-3, QZS-4	Vespucci
11:02:33 - 11:03:33	QZS-2, QZS-3, QZS-4, Vespucci	QZS-1

This section verifies the supplementary effect of joint positioning on constellations. Table. 1 lists tow periods of QZSS and GPS III satellites visible in Xi'an. With the elevation of QZS-1 reduced to almost 10 degrees, L1C of the QZSS-only can still be used for autonomous positioning at 8:34, as shown in Fig. 4. It can be seen from the skyplot that the QZSS satellites are generally concentrated in the southeast direction of the observation site. Influenced by the geometric configuration of the constellation, the positioning error is gigantic in the east (E) direction. Soon after, SDR using L1C signal lost its positioning ability

because barely the remaining 3 satellites were visible in the QZSS-only constellation. The SDR using the GPS III + QZSS L1C joint positioning method restored the positioning capability at 11:02, although the PDOP value became worse than at 8:34, as shown in Fig. 5. Since the satellites are generally concentrated at a higher elevation, the positioning results show a large deviation in the up (U) direction.

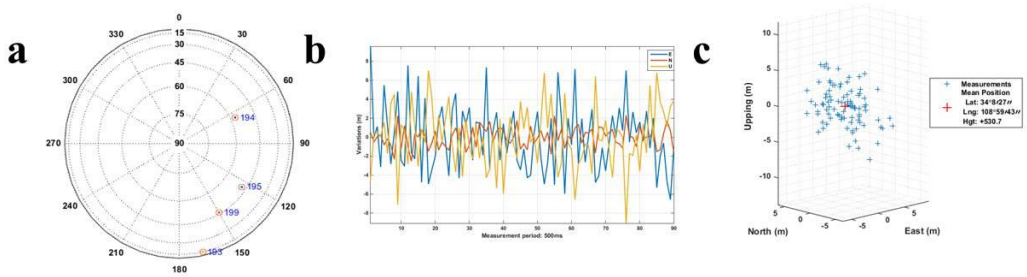

Fig. 4 Positioning results of data collected in Xi'an at 8:34:28 (PDOP = 9.604): **a** the skyplot, **b** the variation in East (E), North (N) and Up (U), **c** the positioning result in the 3D map

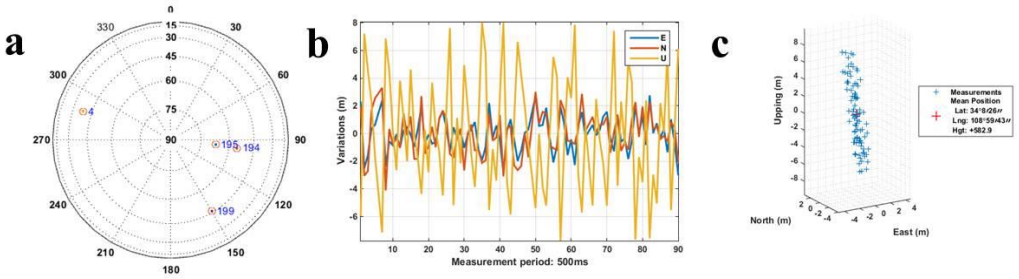

Fig. 5 Positioning results of data collected in Xi'an at 11:02:33 (PDOP = 13.848): **a** the skyplot, **b** the variation in East (E), North (N) and Up (U), **c** the positioning result in the 3D map

Positioning error

The signal collected in Sanya when five satellites are simultaneously visible is used to compare the positioning performance of GPS III + QZSS and QZSS-only. By use of the same correlator spacing (0.1 chips), the three-dimensional positioning error of TMBOC(6,1,4/33) and BOC(1,1) is given in Fig. 6, respectively using the constellations of GPS III + QZSS or QZSS-only. The positioning error is averaged by 2000 positioning samples. Whether using joint positioning or QZSS-only positioning, the positioning error of TMBOC(6,1,4/33) is generally superior to BOC(1,1) in three dimensions. At 15 seconds, the positioning performance of the signal is affected by the environment which may include multipath and signal distortion. It can be seen that TMBOC(6,1,4/33)

shows better resistance at this time. Regardless of whether TMBOC(6,1,4/33) or BOC(1,1) is used, the positioning error of joint positioning is little than that of QZSS-only in three dimensions. This is the result of joint positioning optimizing the constellation composition while reducing the PDOP from 11.22 to 6.45. Since the SDR cannot obtain a priori-position information, the position coordinates must be zeroed at the initial of regression, which results in a large positioning error in the initial stage.

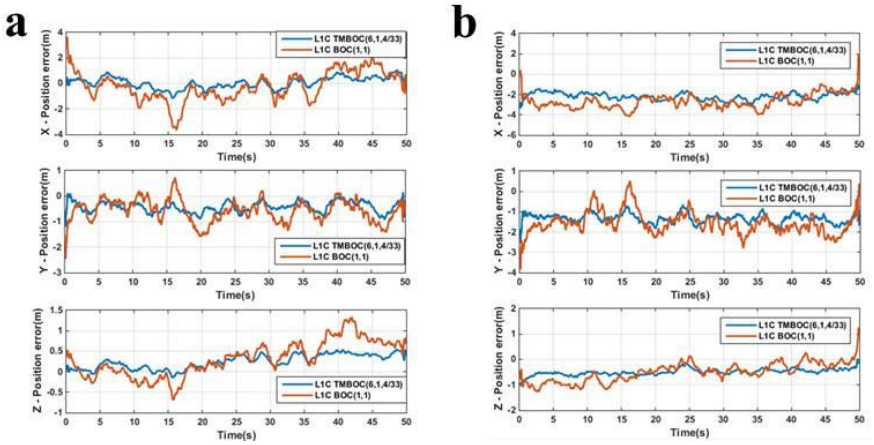

Fig. 6 Position error (correlator spacing = 0.1 chips) : **a** position error from GPS III + QZSS (PDOP = 6.45), **b** position error from QZSS-only (PDOP = 11.22)

Figure 7 shows the positioning error of several user receivers with different correlation spacing. Although the positioning error of TMBOC(6,1,4/33) deteriorated at 0.175 chips, the positioning error at 0.4 chips was significantly restored, as shown in Fig. 7a. As shown in Fig. 7b, the positioning error increases with the correlator spacing for BOC (1,1).

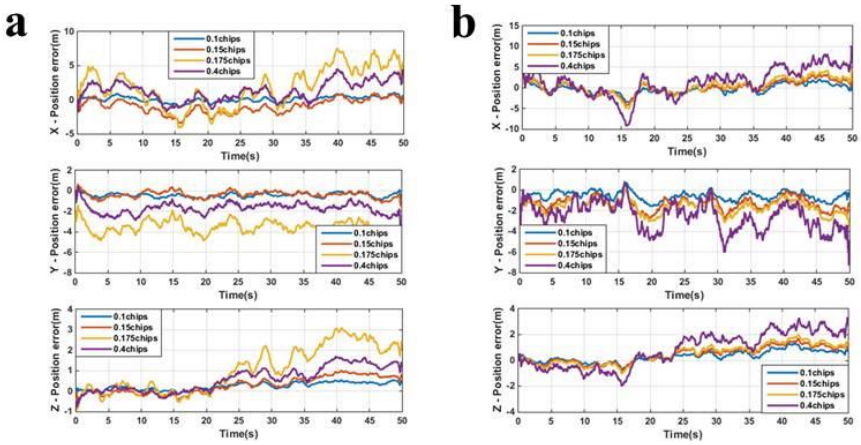

Fig. 7 Position error (GPS III + QZSS) : **a** position error from L1CP when using different correlator spacing, **b** position error from L1CD when using different correlator spacing

Summary and conclusions

The transmission of the new navigation signal leads to the need to verify its positioning performance. This paper proposes a method for SDR to use L1C signal for joint positioning. And the evaluation methodology is proposed for the results using on-air signals. In this paper, the experiments of Xi'an adopted the L1C signal transmitted by the first GPS III satellite, Vespucci, to verify the positioning performance. The joint positioning results prove that the QZSS L1C signal has the claimed enhancement and supplement effect on GPS. This paper gives a direct comparison of GPS III + QZSS joint positioning vs. QZSS-only using on-air signals collected in Sanya. Due to the optimization of the constellation configuration, the positioning error of joint positioning is reduced. Meanwhile, the positioning results using different correlator spacing verify that the poor selection of correlator spacing will affect the positioning result. But properly selecting the correlator spacing allows the positioning performance of TMBOC(6,1,4/33) outperforms that of BOC(1,1).

References

1. C. D. Flynn, A. M. McCaffrey, P. T. Jayachandran, R. B. Langley. (2019). Discovery of new code interference phenomenon in GPS observables. *GPS Solutions*, 23, 65.
2. P. Voosen. (2017). GPS satellites yield space weather data. *Science*, 355, 443.
3. N. Nadarajah, A. Khodabandeh, P. J. G. Teunissen. (2016). Assessing the IRNSS L5-signal in combination with GPS, Galileo, and QZSS L5/E5a-signals for positioning and navigation. *GPS Solutions*,20, 289-297.
4. JAXA. (2018). Interface specification for QZSS, Japan Aerospace Exploration Agency.
5. NAVSTAR Global Positioning System Space Segment / User Segment L1C Interfaces. (2018). IS-GPS-800E.
6. Lee, Chiawei, Chen, Yu-Hsuan, Wong, Gabriel, Lo, Sherman, Enge, Per. (2013). Multipath Benefits of BOC vs. BPSK Modulated Signals Using On-Air Measurements. *Proceedings of the 2013 International Technical Meeting of The Institute of Navigation*, pp. 742-751.
7. J. J. Rushanan. (2007). The Spreading and Overlay Codes for the L1C Signal. *Navigation*,54, 43-51.
8. Fine, Paul, Wilson, Warren. (1999). Tracking Algorithm for GPS Offset Carrier Signals. *Proceedings of the 1999 National Technical Meeting of The Institute of Navigation*, pp. 671-676.